

Spin Dynamics in the Stripe Phase of the Cuprate Superconductors

Brian Møller Andersen and Per Hedegård

Ørsted Laboratory, Niels Bohr Institute, Universitetsparken 5, 2100 Copenhagen Ø, Denmark

(Received 2 November 2004; published 14 July 2005)

Within a model that supports stripe spin and charge order coexisting with a $d_{x^2-y^2}$ -wave superconducting phase, we study the self-consistently obtained electronic structure and the associated transverse dynamical spin susceptibility. In the coexisting phase of superconducting and static stripe order, the resulting particle-hole continuum can strongly damp parts of the low-energy spin-wave branches. This provides insight into recent inelastic neutron scattering data revealing the dispersion of the low-energy collective magnetic modes of lanthanum based cuprate superconductors.

DOI: 10.1103/PhysRevLett.95.037002

PACS numbers: 74.72.-h, 74.25.Ha, 74.25.Jb, 75.40.Gb

The electronic properties of the underdoped cuprates are dominated by competing instabilities and coexistence of several ordered states. An example is given in the accumulating evidence the doped holes tend to self-organize into one-dimensional rivers of charge [1].

For instance, in Nd-doped $\text{La}_{2-x}\text{Sr}_x\text{CuO}_4$ neutron scattering (NS) revealed a quartet of incommensurate (IC) elastic magnetic peaks at $((1 \pm \delta)\pi, \pi)$, $(\pi, (1 \pm \delta)\pi)$ and Bragg charge peaks at $(\pm 2\pi\delta, 0)$, $(0, \pm 2\pi\delta)$ [2]. This is consistent with the doped holes forming 1D domain walls oriented along the Cu-O bonds in the CuO_2 planes. These stripes are separated by $1/\delta$ (in units of the lattice spacing a) and the staggered magnetization gains an extra phase shift π when crossing a stripe. Later, it was realized that d -wave superconductivity (dSC) coexists with the static stripe order [3]. The NS results from pure $\text{La}_{2-x}\text{Sr}_x\text{CuO}_4$ (LSCO) exhibit similar IC peaks [4]. For these materials, Bragg peaks are observed for $0.02 < x < 0.13$, whereas for $x > 0.13$ a small doping dependent spin gap opens in the magnetic excitation spectrum [5].

The dispersion of the IC peaks, i.e., $\delta(\omega)$, between 0–40 meV in optimally and underdoped LSCO was measured recently by Christensen *et al.* [6]. It was found that both in the pseudogap and dSC state, the IC peaks disperse toward (π, π) as the energy increases but with no sign of an intense resonance feature at (π, π) . Furthermore, the IC peaks broaden as the energy increases. A similar dispersion was found in $\text{La}_{2-x}\text{Ba}_x\text{CuO}_4$ by Tranquada *et al.* [7]. In $\text{La}_{2-x}\text{Ba}_x\text{CuO}_4$ and $\text{YBa}_2\text{Cu}_3\text{O}_{6+x}$ it was further found that above the (π, π) crossing, the spin response is dominated by four peaks rotated $\pi/4$ relative to the low-energy IC peaks [7,8]. These high-energy peaks disperse to larger wave vectors with increasing energy transfer. In YBCO the low-energy spin response is dominated by the commensurate (C) (π, π) resonance which disperses downward with decreasing energy [9]. This points to a degree of ubiquity in the spin fluctuation spectrum of the cuprates. The main difference between the materials appears to be the size of the doping dependent spin gap and the intensity distribution along the spin branches. These experiments have

sparked new theoretical studies dealing mostly with the high-energy response [10].

In this Letter we report the self-consistent results of the electronic structure and the corresponding transverse spin susceptibility within a model that supports static IC spin and charge density wave solutions. In particular, we focus on the low-energy spin dynamics and the influence of the dSC on the intensity distribution of the spin branches when it coexists with static spin and charge order. These studies are motivated by the above-mentioned new experimental insight and the strong evidence for stripes in the lanthanum based materials. A similar approach was used to study the phonon anomalies caused by collective modes in the stripe phase of the 2D Hubbard model without allowing for dSC order [11].

Several previous studies of magnetic modes in d -wave superconductors have started from *spatially homogeneous* phases [12,13]. In contrast, recent spin-only models have also been proposed to describe the spin dynamics in the IC stripe phase [14]. Here, we bridge these two apparently complementary approaches by solving self-consistently the following minimal 2D lattice model

$$\hat{H} = - \sum_{\langle ij \rangle \sigma} (t_{ij} \hat{c}_{i\sigma}^\dagger \hat{c}_{j\sigma} + \text{H.c.}) + \sum_{i\sigma} (U \langle \hat{n}_{i\bar{\sigma}} \rangle - \mu) \hat{n}_{i\sigma} + \sum_{\langle ij \rangle} (\Delta_{ij} \hat{c}_{i1}^\dagger \hat{c}_{j1}^\dagger + \text{H.c.}) \quad (1)$$

Here, $\hat{c}_{i\sigma}^\dagger$ creates an electron of spin σ on site i , $t_{ij} = t, t'$ denote the first and second nearest neighbor hopping integrals, μ is the chemical potential, and $\hat{n}_{i\sigma} = \hat{c}_{i\sigma}^\dagger \hat{c}_{i\sigma}$ is the number operator on site i . The model (1) is the mean-field version of the extended Hubbard model with on site repulsion U and nearest neighbor attraction V and is aimed to mimic essential features of phases of coexisting spin, charge, and dSC order. The nearest neighbor attraction V triggers the singlet dSC at the mean-field level, $\Delta_{ij} = V(\langle \hat{c}_{i1} \hat{c}_{j1} \rangle - \langle \hat{c}_{i1} \hat{c}_{j1} \rangle)$. This approach has previously been used extensively to gain insight into the electronic structure in phases of coexisting order [15,16].

As is well known, away from half filling the Hamiltonian (1) produces inhomogeneous spin and charge

order $S_i^z = \frac{1}{2}(\langle \hat{n}_{i\uparrow} \rangle - \langle \hat{n}_{i\downarrow} \rangle)$ and $\rho_i = (\langle \hat{n}_{i\uparrow} \rangle + \langle \hat{n}_{i\downarrow} \rangle)$ with the modulation period of S_i^z being exactly twice the period of ρ_i . This is the stripe phase at the mean-field level. In general, i.e., when $t' \neq 0$, the stripes are metallic since the midgap states cross the Fermi level [16].

For an ordered array of stripes with spin periodicity N we can divide the real-space lattice into smaller supercells of size N . Then, the Hamiltonian can be diagonalized by the Bogoliubov transformation, $\hat{c}_{i\sigma}^\dagger = \sum_{n\mathbf{k}} [u_{n\mathbf{k}\sigma}^*(\mathbf{r}_i) \times e^{-i\mathbf{k}\cdot\mathbf{R}_i} \hat{\gamma}_{n\mathbf{k}\sigma}^\dagger + \sigma v_{n\mathbf{k}\bar{\sigma}}(\mathbf{r}_i) e^{i\mathbf{k}\cdot\mathbf{R}_i} \hat{\gamma}_{n\mathbf{k}\bar{\sigma}}]$, where \mathbf{r}_i denotes a site within the supercell which in turn is positioned at \mathbf{R}_i . The wave vectors \mathbf{k} belong to the corresponding reduced Brillouin zone, and $\sigma = +(-)1$ for up(down) spin. This results in a set of Bogoliubov–de Gennes equations to be diagonalized for each \mathbf{k} . The self-consistency is enforced through iteration of the relations, $1 - n_h = \frac{1}{N} \sum_{i\sigma} \langle \hat{n}_{i\sigma} \rangle$, n_h is the hole doping, and

$$\langle \hat{n}_{i\sigma} \rangle = \sum_{n\mathbf{k}} [|u_{n\mathbf{k}\sigma}(i)|^2 f(E_{n\mathbf{k}\sigma}) + |v_{n\mathbf{k}\bar{\sigma}}(i)|^2 f(-E_{n\mathbf{k}\bar{\sigma}})], \quad (2)$$

$$\Delta_{ij} = \sum_{n\mathbf{k}} [v_{n\mathbf{k}\sigma}^*(i) u_{n\mathbf{k}\sigma}(j) f(E_{n\mathbf{k}\sigma}) - u_{n\mathbf{k}\sigma}(i) v_{n\mathbf{k}\sigma}^*(j) f(-E_{n\mathbf{k}\sigma})]. \quad (3)$$

As usual, $f(E) = [1 + \exp(E\beta)]^{-1}$ denotes the Fermi distribution function with $\beta = 1/kT$.

Below, we report the spin dynamics obtained from the stable configurations both with and without dSC when $U = 4.0t$, $n_h = 0.125$, and $N = 8$. In principle, for a given set of parameters U , V , t' , and n_h the system may prefer a spin period different from $N = 8$. By varying n_h we have checked that this possibility does not qualitatively alter the results below.

A typical example of the self-consistent results for the spin (charge) density S_i^z (ρ_i) and the pairing potential $\Delta_i^d = (\Delta_{i,i+e_x} + \Delta_{i,i-e_x} - \Delta_{i,i+e_y} - \Delta_{i,i-e_y})/4$ is shown in Fig. 1(a). Clearly, this shows the expected antiphase stripe ordering with concomitant modulations of Δ_i^d . The bond-centered solutions are found to have energies slightly lower than the site-centered stripes.

Turning briefly to the electronic structure obtained from these self-consistent solutions, it is well known that for the spectral weight, $I(\mathbf{k}) = \int_{\mu-\Delta w}^{\mu} A(\mathbf{k}, \omega) d\omega$, the stripes generate weight around the antinodal regions [16,17].

Here $A(\mathbf{k}, \omega)$ is the single-particle spectral function and Δw is an integration window below the chemical potential μ . For instance, in Fig. 1(b) we show $I(\mathbf{k})$ for $0 \leq k_x, k_y \leq \pi$ for the same parameters used in Fig. 1(a) but allowing for stripe disorder [18]. This figure is strikingly similar to the recent ARPES data by Zhou *et al.* [19]. Furthermore, the stripe ordering causes a modulation of the pairing potential as seen in Fig. 1(a) which influences the Fourier transform of the local density of states (LDOS) $N_{\mathbf{q}}(\omega)$ [16,20]. For instance, as seen from Fig. 1(c), the real part of $N_{\mathbf{Q}^*}(\omega)$ versus energy ω at the charge ordering vector $\mathbf{Q}^* = (\frac{3\pi}{2}, 0)$ exhibits two low-energy zero crossings in agreement with recent STM measurements by Howald *et al.* [21].

Motivated by the agreement of the self-consistent mean-field solutions of Eq. (1) and the mentioned electronic probes, we turn now to our main topic: the collective spin dynamics in the stripe phase. The stripes explicitly break the SU(2) spin rotation symmetry and hence associated Goldstone modes are expected in the transverse spin susceptibility $\chi^{+-}(\mathbf{q}, \omega)$. Below, we investigate the effect of the charges and the dSC order on the dynamic part of the spin modes. An explicit calculation of the Fourier transform of $\chi^{+-}(\mathbf{r}_i, \mathbf{r}_j, \tau) = -\langle T_\tau \hat{S}_j^+(\tau) \hat{S}_i^-(0) \rangle$ shows that to Gaussian order the response is given by the diagonal elements of the following $N \times N$ matrix

$$\chi^{+-}(\mathbf{q}, \omega) = \chi_0^{+-}(\mathbf{q}, \omega) [1 - U \chi_0^{+-}(\mathbf{q}, \omega)]^{-1}. \quad (4)$$

The matrix elements of the bare susceptibility $\chi_0^{+-}(\mathbf{q}, \omega)_{\mathcal{Q}\mathcal{Q}'}$ are given by

$$\begin{aligned} \chi_0^{+-}(\mathbf{q}, \omega)_{\mathcal{Q}\mathcal{Q}'} = & \frac{1}{4N^2} \sum_{\substack{\mathbf{k}m\mathbf{l} \\ \mathbf{r}_i \mathbf{r}_j \sigma}} \left[a_1(u, v) \frac{1 - f(E_{n\mathbf{k}\sigma}) - f(E_{m\mathbf{k}+\mathbf{q}\sigma})}{\omega + E_{m\mathbf{k}+\mathbf{q}\sigma} + E_{n\mathbf{k}\sigma} + i\Gamma} \right. \\ & + a_2(u, v) \frac{f(E_{n\mathbf{k}\sigma}) + f(E_{m\mathbf{k}+\mathbf{q}\sigma}) - 1}{\omega - E_{m\mathbf{k}+\mathbf{q}\sigma} - E_{n\mathbf{k}\sigma} + i\Gamma} \\ & + b_1(u, v) \frac{f(E_{n\mathbf{k}\sigma}) - f(E_{m\mathbf{k}+\mathbf{q}\bar{\sigma}})}{\omega + E_{m\mathbf{k}+\mathbf{q}\bar{\sigma}} - E_{n\mathbf{k}\sigma} + i\Gamma} \\ & \left. + b_2(u, v) \frac{f(E_{m\mathbf{k}+\mathbf{q}\sigma}) - f(E_{n\mathbf{k}\bar{\sigma}})}{\omega + E_{n\mathbf{k}\bar{\sigma}} - E_{m\mathbf{k}+\mathbf{q}\sigma} + i\Gamma} \right] \\ & \times e^{i\mathbf{q}\cdot(\mathbf{r}_j - \mathbf{r}_i) + i\mathbf{Q}\cdot\mathbf{r}_j - i\mathbf{Q}'\cdot\mathbf{r}_i}, \quad (5) \end{aligned}$$

where \mathbf{Q} are N reciprocal lattice vectors of the supercell lattice. The coefficients $a_1(u, v)$ and $b_1(u, v)$ are given by the

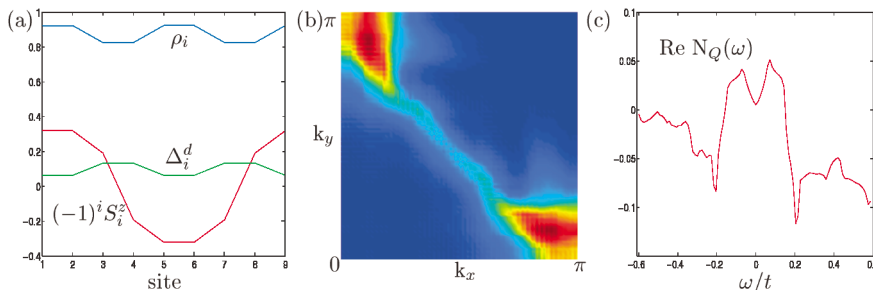


FIG. 1 (color online). (a) Bond-centered spin density $(-1)^i S_i^z$ (red), charge density ρ_i (blue), and pairing potential Δ_i^d (green) vs site obtained when $U = 4.0t$, $V = 2.0t$, $t' = -0.37t$; (b) the spectral weight $I(\mathbf{k})$ ($\Delta w = 0.1t$) vs \mathbf{k} for disordered stripes. (c) Plot of the real part of $N_{\mathbf{Q}^*}(\omega)$ vs energy ω .

following combinations of the coherence factors u and v

$$a_1(u, v) = v_{nk\sigma}^*(\mathbf{r}_i)u_{m\mathbf{k}+\mathbf{q}\sigma}(\mathbf{r}_i)[v_{nk\sigma}(j)u_{m\mathbf{k}+\mathbf{q}\sigma}^*(\mathbf{r}_j) - u_{nk\sigma}(\mathbf{r}_j)v_{m\mathbf{k}+\mathbf{q}\sigma}^*(\mathbf{r}_j)], \quad (6)$$

$$b_1(u, v) = u_{nk\sigma}^*(\mathbf{r}_i)u_{m\mathbf{k}+\mathbf{q}\bar{\sigma}}(\mathbf{r}_i)[u_{nk\sigma}(\mathbf{r}_j)u_{m\mathbf{k}+\mathbf{q}\bar{\sigma}}^*(\mathbf{r}_j) + v_{nk\sigma}(\mathbf{r}_j)v_{m\mathbf{k}+\mathbf{q}\bar{\sigma}}^*(\mathbf{r}_j)]. \quad (7)$$

These coefficients are independent of the reciprocal vectors \mathbf{Q} since the eigensystem of the Hamiltonian for a given \mathbf{k} is invariant under shifts $\mathbf{k} \rightarrow \mathbf{k} \pm \mathbf{Q}$. The remaining factors, $a_2(u, v)$ and $b_2(u, v)$, are obtained from $a_1(u, v)$ and $b_1(u, v)$ by interchanging $u_\sigma \leftrightarrow v_\sigma$ and $u_\sigma \leftrightarrow v_{\bar{\sigma}}$, respectively. In Eq. (5), the real-space sum $\mathbf{r}_i, \mathbf{r}_j$, extends over a single supercell of size N whereas \mathbf{k} belongs to the reduced Brillouin zone (BZ). Below, we set $kT = \Gamma = 0.005t$. Because of the large number of diagonalizations involved in the sum in Eq. (5), we are unfortunately unable to obtain high-resolved 2D constant energy cuts through the BZ. However, as shown below, the explicit ω dependence in Eq. (5) allows us to calculate, e.g., (q_x, ω) plots.

Without spin order ($U = 0$), the expression (5) reduces to the well-known result for a homogeneous d -wave BCS superconductor [13]. Further, when $n_h = 0$ and $V = 0$ but $U \neq 0$ we find the antiferromagnetic (AF) state and its expected acoustic spin cones pivoted at (π, π) . The spin branches are determined by the poles of Eq. (4) which in the homogeneous case is given by the usual condition: $U \text{Re} \chi_0^{+-}(\mathbf{q}, \omega) = 1$. This condition is no longer valid due to the $N \times N$ matrix structure of Eq. (4). In the insulating stripe phase without dSC, ($t' = V = 0$), we show in Fig. 2(a) the imaginary part of the full spin susceptibility. Clearly, the state contains the expected Goldstone modes shifted to $(\pi(1 \pm 2/N), \pi)$ [14]. The higher harmonics (not shown) have negligible weight compared to the main $(\pi(1 \pm 2/N), \pi)$ modes. The branches broaden and lose intensity as the energy is increased leaving very small weight near (π, π) . At low energy, the 2D dispersion as found in constant energy scans with $q_y \neq 0$ is dominated by circular spin cones pivoted at the IC points.

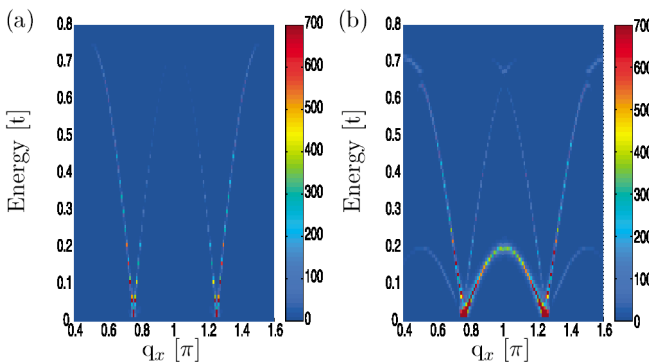


FIG. 2 (color online). Imaginary part of the full spin susceptibility $\text{Im} \chi^{+-}(q_x, q_y, \omega)$ at $q_y = \pi$ for $N = 8$, $U = 4.0t$, $V = 0.0t$, and $t' = 0.0$ (a) and $t' = -0.4t$ (b).

There will be four cones when the vertical/horizontal stripe domains are equally distributed. There is an energy range where the cones merge and form weak intensity maxima at positions rotated $\pi/4$ from the Bragg IC points. In the range $-0.3 < t' < 0.0$, the spin susceptibility is similar to Fig. 2(a). However, in the metallic stripe phase ($t' < -0.3$), nesting conditions support an additional collective mode as defined from the poles of Eq. (4). In Fig. 2(b) we show the special case where this mode has (nearly) softened. For other values of t' it becomes fully dynamic and moves to higher energy.

The results in Fig. 2 illustrate a general problem that also applies to the spin-only approaches [14]: the outer branches, i.e., at $|q_x - \pi| > 2\pi/N$, are *not observed* in the low-energy NS data [4,6]. This is contrary to the non-superconducting $\text{La}_{2-x}\text{Sr}_x\text{NiO}_4$ where all four spin branches can be clearly seen in constant energy cuts through the BZ [22]. In our model, the intensity along the spin branches increases monotonically when lowering the energy since the low-energy part of $\text{Im} \chi_0^{+-}(\mathbf{q}, \omega)_{QQ'}$ is largely independent on the wave vector \mathbf{q} .

What happens when superconductivity is included? Then, we expect the matrix elements $\chi_0^{+-}(\mathbf{q}, \omega)_{QQ'}$ to strongly depend on \mathbf{q} at low energy. Indeed, in the homogeneous dSC phase the particle-hole continuum continues to $\omega = 0$ for wave vectors connecting the nodes of the d -wave gap. In Fig. 3 we show representative results for $\text{Im} \chi^{+-}(\mathbf{q}, \omega)$ in the coexisting phase. In the low $|t'|$ regime, the result is similar to Fig. 2(a). However, for parameters similar to those used in Fig. 1 ($-0.4 < t' < -0.3$), the result is very different as shown in Fig. 3(b). The spin response consists of two branches: a high-energy branch that is damped when $|q_x - \pi| < 2\pi/N$ and a low-energy branch strongly damped when $|q_x - \pi| > 2\pi/N$. As mentioned, the latter result is an important feature of the NS experiments on LSCO [6]. This result is one of the main points of this Letter. It is not sensitive to the size of the resulting gap Δ , but rather to the specific band structure similar to the situation of a homogeneous dSC. Another effect induced by V is the weight around (π, π) which is

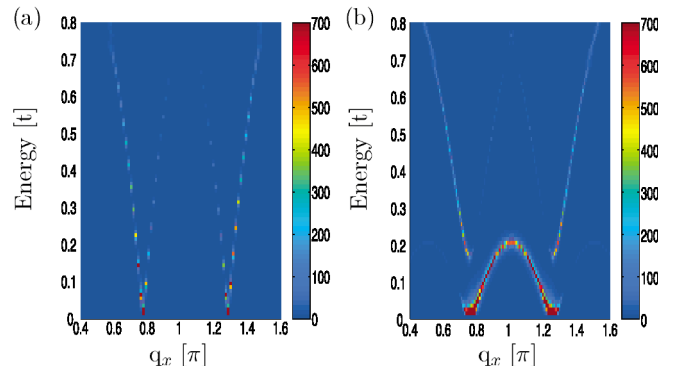


FIG. 3 (color online). $\text{Im} \chi^{+-}(q_x, q_y, \omega)$ at $q_y = \pi$ for $N = 8$, $U = 4.0t$, $V = 2.0t$, and $t' = -0.2t$ (a) and $t' = -0.37t$ (b). The parameters in (b) are identical to those used in Fig. 1

significantly increased in the dSC phase. Note that the overall form of the spin fluctuation spectrum of Fig. 3(b) has the characteristic hourglass shape [7,9].

In the present approach we calculate the spin response in the static stripe phase relevant in the underdoped regime where a pseudogap is known to exist above T_c . Thus, the “normal” state spin susceptibility in this doping region is expected to be more like a thermally broadened version of Fig. 3(b) as opposed to the results in Fig. 2. In the optimally doped regime a spin gap opens due to the fluctuating nature of the stripes and we expect the intensity of the IC modes to redistribute to slightly above the spin gap [6]. In the far overdoped regime the stripes presumably disintegrate and the picture presented here eventually breaks down.

For other periodicities N we find that at fixed U the spin-wave velocity is largely unchanged. Hence, the energetic position E_{res} of the (π, π) “resonance” is mainly determined by the stripe separation. This means that E_{res} increases with the doping in the underdoped regime. This is unlike the homogeneous dSC ($U = 0, V \neq 0$) where the intensity at (π, π) can be increased by band-structure nesting, but where E_{res} is solely determined by the maximum value of the dSC gap Δ which, contrary to experiments, decreases as the doping increases.

Finally, note that even though the downward mode dispersion at low energy [Fig. 3(b)] is qualitatively similar to that found in a pure dSC state, the intensity distribution of the spin branch is reversed [13]. In the homogeneous dSC state (mainly aimed at modeling YBCO and BSCCO) the intensity is maximum at (π, π) and decreases with decreasing energy until it merges with the continuum. At lower energies the response is completely void due to the opening of a spin gap.

In summary, we have calculated the electronic structure and the associated dynamical spin susceptibility in the stripe phase of Eq. (1). We find that self-consistent solutions reproduce salient features of widely different experimental probes including ARPES, STM, and low-energy NS indicating that the stripe phase is a good starting point for describing the LSCO materials. In the coexisting phase of spin, charge, and dSC order, the outer low-energy spin modes are found to be strongly damped. In the future, it will be interesting to study in more detail the dispersion of the high-energy spin fluctuations within the present approach.

This work is supported by the Danish Technical Research Council via the Framework Programme on Superconductivity.

[1] J. Zaanen and O. Gunnarson, Phys. Rev. B **40**, 7391 (1989); D. Poilblanc and T.M. Rice, *ibid.* **39**, R9749 (1989); K. Machida, Physica (Amsterdam) **158C**, 192 (1989); H.J. Schulz, J. Phys. (Paris) **50**, 2833 (1989).

[2] J.M. Tranquada *et al.*, Nature (London) **375**, 561 (1995).
 [3] J.M. Tranquada *et al.*, Phys. Rev. Lett. **78**, 338 (1997).
 [4] S.-W. Cheong *et al.*, Phys. Rev. Lett. **67**, 1791 (1991).
 [5] H. Kimura *et al.*, Phys. Rev. B **59**, 6517 (1999); S. Wakimoto *et al.*, *ibid.* **60**, R769 (1999); S. Wakimoto, R.J. Birgeneau, Y.S. Lee, and G. Shirane, *ibid.* **63**, 172501 (2001).
 [6] N.B. Christensen *et al.*, Phys. Rev. Lett. **93**, 147002 (2004).
 [7] J.M. Tranquada *et al.*, Nature (London) **429**, 534 (2004).
 [8] S.M. Hayden *et al.*, Nature (London) **429**, 531 (2004).
 [9] M. Arai *et al.*, Phys. Rev. Lett. **83**, 608 (1999); H.A. Mook, P. Dai, and F. Dogan, *ibid.* **88**, 097004 (2002).
 [10] M. Vojta and T. Ulbricht, Phys. Rev. Lett. **93**, 127002 (2004); G.S. Uhrig, K.P. Schmidt, and M. Grüninger, *ibid.* **93**, 267003 (2004); G. Seibold and J. Lorenzana, Phys. Rev. Lett. **94**, 107006 (2005); M. Vojta and S. Sachdev, “Proceedings of SNS 2004, Sitges, Spain,” cond-mat/0408461; I. Eremin *et al.*, Phys. Rev. Lett. **94**, 147001 (2005).
 [11] E. Kaneshita, M. Ichioka, and K. Machida, Phys. Rev. Lett. **88**, 115501 (2002).
 [12] Q. Si, Y. Zha, K. Levin, and J.P. Lu, Phys. Rev. B **47**, 9055 (1993); T. Dahm, D. Manske, and L. Tewordt, *ibid.* **58**, 12454 (1998); A.V. Chubukov, B. Janko, and O. Tchernyshyov, *ibid.* **63**, 180507(R) (2001); F. Onufrieva and P. Pfeuty, *ibid.* **65**, 054515 (2002); D.K. Morr and D. Pines, Phys. Rev. Lett. **81**, 1086 (1998); J. Brinckmann and P.A. Lee, *ibid.* **82**, 2915 (1999).
 [13] N. Bulut and D.J. Scalapino, Phys. Rev. B **47**, 3419 (1993); M.R. Norman, Phys. Rev. B **63**, 092509 (2001).
 [14] C.D. Batista, G. Ortiz, and A.V. Balatsky, Phys. Rev. B **64**, 172508 (2001); F. Krüger and S. Scheidl, *ibid.* **67**, 134512 (2003); E.W. Carlson, D.X. Yao, and D.K. Campbell, *ibid.* **70**, 064505 (2004).
 [15] Y. Chen and C.S. Ting, Phys. Rev. Lett. **92**, 077203 (2004); J.-X. Zhu, I. Martin, and A.R. Bishop, Phys. Rev. Lett. **89**, 067003 (2002).
 [16] M. Ichioka and K. Machida, J. Phys. Soc. Jpn. **68**, 4020 (1999); **71**, 1836 (2002).
 [17] M.I. Salkola, V.J. Emery, and S.A. Kivelson, Phys. Rev. Lett. **77**, 155 (1996); M. Granath, V. Oganessian, D. Orgad, and S.A. Kivelson, Phys. Rev. B **65**, 184501 (2002).
 [18] The stripes are disordered with a flat distribution of average stripe distance of four lattice constants. Figure 1(b) is symmetrized around $k_x = k_y$ assuming that vertical/horizontal stripes contribute evenly. As discussed by Granath *et al.* [17] the ordered array already contains the essentials of Fig. 1(b) except from the ghostly nodal weight.
 [19] X.J. Zhou *et al.*, Phys. Rev. Lett. **86**, 5578 (2001).
 [20] D. Podolsky, E. Demler, K. Damle, and B.I. Halperin, Phys. Rev. B **67**, 094514 (2003).
 [21] C. Howald, H. Eisaki, N. Kaneko, M. Greven, and A. Kapitulnik, Phys. Rev. B **67**, 014533 (2003).
 [22] P. Bourges, Y. Sidis, M. Braden, K. Nakajima, and J.M. Tranquada, Phys. Rev. Lett. **90**, 147202 (2003); A.T. Boothroyd *et al.*, Phys. Rev. B **67**, 100407(R) (2003).